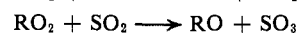


absorbed light intensity was normally about 0.2  $\mu$ /sec, the rate constants  $k_{10}$  and  $k_{12}$  can be estimated to be greater than  $10^8 M^{-1} \text{sec}^{-1}$  since even a few microns of either NO or NO<sub>2</sub> were found to scavenge all the CH<sub>3</sub>O<sub>2</sub> radicals and completely suppress reaction 6. The peak radiation intensity in the lower atmosphere is about  $2 \times 10^{16}$  photons/(cm<sup>2</sup> sec) for radiation between 3000 and 4000 Å. The average absorption coefficient (to base 10) of the principal absorbing gas, NO<sub>2</sub>, is about  $100 M^{-1} \text{cm}^{-1}$ . Thus the absorbed intensity in the lower atmosphere is given by  $I_a = 0.33 \times 10^{-2} [\text{NO}_2]$ , where [NO<sub>2</sub>] is in  $M$  units and  $I_a$  is in units of  $M \text{sec}^{-1}$ . For concentrations of NO<sub>2</sub> greater than  $10^{-10} M$  (greater than  $2 \times 10^{-3}$  ppm), the concentration of CH<sub>3</sub>O<sub>2</sub> radicals must be less than  $10^{-12} M$  even if one in every 100 photodecompositions of NO<sub>2</sub> produced a CH<sub>3</sub>O<sub>2</sub> radical (an overestimate). Using  $k_8$  and  $k_{12}$ , it is seen that even at this high upper limit for CH<sub>3</sub>O<sub>2</sub> concentration, reaction 6 is still slower than reaction 12. Since air pollution concentrations of NO<sub>2</sub> are much greater (about 0.1 ppm) than  $10^{-10} M$ , reaction 6 can be of no consequence in urban air pollution.

Since radical reactions cannot compete with reactions

10 or 12, perhaps other pollutants are competing for peroxy radicals. Two likely candidates are CO and SO<sub>2</sub>



Neither of these reactions has been reported previously. They are currently under study in our laboratory.

Finally one must consider the possibility of the photodissociation of the molecules produced in reactions 10 and 12 (nitrates, peroxy nitrates, and peroxy nitrates) as sources of alkoxy radicals. Assuming these molecules have absorption coefficients similar to NO<sub>2</sub>, then the lifetime of these molecules to photodissociation can be computed from  $I_a$  to be  $3 \times 10^2 \text{sec}$  ( $\sim 5 \text{min}$ ) for peak intensities. This is certainly rapid enough to be important in the atmosphere. Therefore the absorption spectra and absorption coefficients of these compounds must be determined to test this possibility.

**Acknowledgment.** This work was supported by the Environmental Protection Agency through the Office of Air Programs under Grants No. AP 01044 and AP 00022, for which we are grateful.

## Primary Processes in the Photochemistry of 1-Pyrazoline

G. L. Loper and F. H. Dorer\*

*Contribution from the Chemistry Department,  
California State University—Fullerton, Fullerton, California 92634.  
Received July 5, 1972*

**Abstract:** The fluorescence decay times and quantum yields for emission from 1-pyrazoline in the gas phase decrease with increasing vibronic energy. While the radiative lifetime is virtually independent of excitation energy, the nonradiative lifetime decreases at higher energies. When  $\lambda_{\text{ex}}$  is shorter than 308 nm 1-pyrazoline decomposes with unit quantum efficiency in less than 10 nsec. Subsequent to its excitation to lower vibronic levels of its first singlet state 1-pyrazoline decomposes with nearly statistical intramolecular energy relaxation in the cyclopropane forming reaction, but there is definitely nonrandom energy relaxation when the molecule decomposes from higher vibronic levels. Oxygen has an efficiency of  $\sim 0.5$  for the quenching of 1-pyrazoline fluorescence. Oxygen appears to remove  $\sim 30 \text{kcal mol}^{-1}$  from the singlet state of 1-pyrazoline to produce a product that behaves like a hot ground state molecule. The utility of using 1-pyrazoline emission to study vibrational energy transfer from its excited singlet state to diluent molecules is demonstrated for the case in which cyclohexane is the deactivator.

The decomposition of 1-pyrazolines is thought to involve trimethylene biradical intermediates, and their photolysis has been used to characterize the reactions of excited trimethylene biradicals.<sup>1-5</sup> In addition, the energy partitioning to the internal degrees of freedom of the cyclopropane fragment produced on photolysis of several of these cyclic azo compounds has been studied in some detail.<sup>6-9</sup> It appears that the

product energy distribution is nonrandom and pressure and wavelength dependent. In order to better interpret the significance of the observed product and energy distribution data, it is necessary to characterize the primary photophysical processes that occur prior to or in competition with the photofragmentation reaction.

Therefore, we have carried out this study of the photochemistry of the simplest of the series of 1-pyrazolines. Since, in the longer wavelength region of excitation to the first singlet band the fluorescence quantum yield is quite high for 1-pyrazoline, we have been able to extend the lifetime and quantum yield measurements to sufficiently low pressures such that collisional relaxation prior to emission or decomposition is of negligible importance.

### Experimental Section

**Materials.** The 1-pyrazoline used in this study was prepared as

(1) R. Moor, A. Mishra, and R. J. Crawford, *Can. J. Chem.*, **46**, 3305 (1968).

(2) E. B. Klunder and R. W. Carr, *Chem. Commun.*, 742 (1971).

(3) S. D. Nowacki, P. B. Do, and F. H. Dorer, *ibid.*, 273 (1972).

(4) D. H. White, P. B. Condit, and R. G. Bergman, *J. Amer. Chem. Soc.*, **94**, 1348 (1972).

(5) L. M. Stephenson and J. I. Brauman, *ibid.*, **93**, 1988 (1971).

(6) T. F. Thomas, C. I. Sutin, and C. Steel, *ibid.*, **89**, 5107 (1967).

(7) F. H. Dorer, *J. Phys. Chem.*, **73**, 3109 (1969).

(8) F. H. Dorer, E. Brown, J. Do, and R. Rees, *ibid.*, **75**, 1640 (1971).

(9) P. Cadman, H. M. Meunier, and A. F. Trotman-Dickenson, *J. Amer. Chem. Soc.*, **91**, 7640 (1969).

described previously.<sup>10</sup> Where appropriate the purity of all chemicals used in this work was ensured by glpc analysis.

Before being transferred to the fluorescence, absorption, or photolysis cells, all samples were deaerated several times at liquid nitrogen temperature on a mercury free greaseless vacuum line. For the emission and absorption measurements, known pressures of gases were measured into the fluorescence cells of known volume by using accurately calibrated volumes in the vacuum line and two Wallace-Tiernan gauges that covered the pressure ranges of 0–18.6 and 0–1500 Torr. A similar procedure was used to load the quartz photolysis cells for the measurement of product compositions and decomposition quantum yields, except that a Pyrex spiral gauge was used for the pressure measurements. For the measurements of the fluorescence quantum yield relative to acetone, the low pressures of 1-pyrazoline were measured out directly by using a MKS Instruments, Inc., Baratron pressure gauge with a Type 77H-30 pressure head.

**Absorption Spectra.** Values for the molar extinction coefficients of 1-pyrazoline at various excitation wavelengths,  $\epsilon_\lambda$ , were calculated from gas-phase absorption spectra taken with a spectral resolution of 1 Å on a Cary 14R spectrophotometer.

**Excitation Spectra.** The optical arrangement used in this work for the study of the high resolution excitation spectra was similar to one employed earlier.<sup>11</sup> The arc from a Hanovia 959 C-98 500-W xenon lamp was focused onto the entrance slit of a 0.75-m grating monochromator (Spex Industries Model 1702,  $f = 6.3$ , 1.1 nm/mm reciprocal dispersion on first order, 500.0 nm blaze). The monochromator was scanned continuously on second order with entrance and exit slit widths of 50  $\mu$  to give a theoretical spectral resolution of  $\sim 0.03$  nm. The dispersed light from the monochromator was then passed through a Corning CS 7-54 uv envelope filter into the center of a T-shaped fluorescence cell. The 1-pyrazoline emission was collected at right angles to the exciting light by a cooled EMI 9558 QB (S-20) photomultiplier tube (PMT) through a silica lens. A Corning CS 0-51 uv blocking filter was placed between the fluorescence T-cell and the PMT. This allowed most of the broad 1-pyrazoline emission profile (340–540 nm) to be viewed, while minimizing the scattered radiation. The output signal from the PMT was fed into the same photon counting system as also described previously.<sup>11</sup>

For maximizing the accuracy of the excitation spectra the results of several scans were averaged. Corrections were made for variation in the incident photon intensity with excitation wavelength as well as "background counts" due to photomultiplier dark current and cell glow from scattered exciting light. The former was obtained by reflecting the monochromator output (including the CS 7-54 filter but with the slits nearly closed) with a 45° mirror into the PMT and by then correcting the observed photon counts as a function of wavelength for the quantum efficiency of the S-20 photocathode sensitivity as specified by the manufacturer. The correct light intensity decreased by only about 9% from  $\lambda_{\text{ex}} = 340.0$  nm to  $\lambda_{\text{ex}} = 310.0$  nm.

**Emission Spectra and Quenching Measurements.** The efficiency with which various molecules quench or enhance the fluorescence of 1-pyrazoline was determined by monitoring the changes in low resolution excitation spectra with added gas pressure. These excitation spectra as well as all emission spectra obtained in this study were run on a Hitachi Perkin-Elmer MPF-2A spectrofluorimeter equipped with a Hamamatsu R106 photomultiplier tube which has a S-19 spectral response. The excitation source was a 150-W Osram XBO-150 xenon lamp. The sample compartment of the spectrofluorimeter was modified to accept a fluorescence T-cell for gas-phase samples. Since the present study does not require that the emission spectra be corrected for the spectral response of the emission monochromator and photomultiplier tube, they are presented here in their uncorrected form.

**Emission Lifetime Measurements.** Emission lifetimes of 1-pyrazoline at various exciting wavelengths were measured directly by a single photon counting, time correlation technique using either a pulsed D<sub>2</sub> or N<sub>2</sub> discharge lamp (TRW nanosecond spectral source 31A) with decay times of  $\sim 1.1$  and 10.8 nsec, respectively. The experimental set-up used for this single photo counting decay fluorimeter was identical with one described in detail earlier.<sup>12</sup> The pulsed exciting light was focused onto the entrance slit of a

small Bausch and Lomb high intensity monochromator (Model 33-86-010). This monochromator (as well as those used in the measurement of the previously described excitation and emission spectra) was calibrated with the 253.7, 312.6, and 313.2 nm mercury lines of a Pen Ray Model SCT 1 quartz lamp. The dispersed light from the monochromator was then focused into the center of a T-shaped fluorescence cell by a relay lens assembly (TRW). The emission was observed at right angles after being focused by another relay lens assembly onto a RCA 8575 VI phototube. No emission filters were in general used so that the entire emission profile could be viewed.

At the excitation wavelengths where the observed photon counts were small it became necessary to subtract the "background counts" obtained with the empty fluorescence cell before plotting the decay. The excitation wavelengths ( $\lambda_{\text{ex}}$ ) and measured  $\tau_F$  values are typically accurate to within  $\sim \pm 0.3$  nm and  $\sim \pm 3\%$ , respectively.

**Decomposition Quantum Yields.** The quantum yield for the decomposition of 1-pyrazoline was measured at 313 nm by using the photolysis of cyclobutanone as an actinometer. The quantum yield for photolysis of cyclobutanone by 313-nm radiation is unity at pressures as high as 20 Torr.<sup>11,18</sup> Three experiments were carried out by photolyzing mixtures of cyclobutanone and 1-pyrazoline. A fourth measurement was made by photolyzing the two separately and continuously recording the excitation beam intensity.

The quantum yield for decomposition of 1-pyrazoline by 333 nm radiation was measured relative to  $\phi_D(313)$ . The relative quantum yields were calculated from the relation

$$\phi_D(333)/\phi_D(313) = (R_p/R_t R_i)(1 - 10^{-\epsilon_{313} C t}) / \sum_{\lambda} (I_{(\lambda)}/I_T)(1 - 10^{-\epsilon_{\lambda} C t}) \quad (1)$$

$R_p$ ,  $R_i$ , and  $R_t$  are the relative amounts of products formed, relative total incident radiation intensity, and relative photolysis times at 333 and 313 nm,  $(I_{(\lambda)}/I_T)$  is the per cent of radiation incident on the cell at wavelength  $\lambda$ ,  $C$  is concentration, and  $\epsilon$  is the molar extinction coefficient. The sum term in the denominator was evaluated in 0.2-nm intervals over the emission spectrum of the B and L monochromator and lamp.

For the decomposition quantum yield measurements the excitation lamp was a 200-W Osram super pressure mercury lamp used in conjunction with a Bausch and Lomb high intensity grating monochromator. In order to obtain the 333-nm radiation, the output of the lamp and monochromator was passed through a Corning CS 7-51 filter. The wavelength-intensity distribution of the excitation radiation was calibrated with a Jarrel-Ash 0.25-m grating monochromator. The wavelength distribution of the exciting radiation was confined to the region between 328 and 339 nm. The average radiation absorbed by the 1-pyrazoline was 333 nm with this setup.

Several measurements were made of the relative quantum yield for decomposition as a function of pyrazoline pressure and diluent pressure using this above arrangement for 333 nm excitation.

**Product Analysis.** The products were analyzed on a Hewlett-Packard 5750 gas chromatograph fitted with a vacuum inlet loop using the flame ionization detector. All products except nitrogen were clearly separated on a 40-ft dimethylsulfolane column.

## Results and Discussion

**Absorption, Excitation, and Emission Spectra.** The gas-phase absorption spectra of 1-pyrazoline exhibits two complex absorption bands: one extending over the wavelength region 337–275 nm ( $\epsilon_{\text{max}} \simeq 533$  l. mol<sup>-1</sup> cm<sup>-1</sup> at 318.4 nm); and another that absorbs weakly from 260 to 220 nm below which it suddenly becomes highly structured and more intense ( $\epsilon_{\text{max}} \simeq 1326$  l. mol<sup>-1</sup> cm<sup>-1</sup> at 209.6 nm). Unfortunately, a detailed spectral analysis and assignment of the vibrational-electronic transitions giving rise to these bands has not been reported. Although the vibrational spectra of 1-pyrazoline are best interpreted in terms of a slightly puckered ( $19.7 \pm 1.0^\circ$ ) equilibrium ground-state geometry,<sup>14</sup> its electronic spectra are probably better understood by

(10) R. J. Crawford, A. Mishra, and R. J. Dummel, *J. Amer. Chem. Soc.*, **88**, 3959 (1966).

(11) J. C. Hemminger and E. K. C. Lee, *J. Chem. Phys.*, **56**, 5284 (1972).

(12) G. M. Breuer and E. K. C. Lee, *J. Phys. Chem.*, **75**, 989 (1971); G. M. Breuer, Ph.D. Thesis, University of California, Irvine, 1972.

(13) N. E. Lee and E. K. C. Lee, *J. Chem. Phys.*, **50**, 2094 (1969).

(14) J. R. Durig, J. M. Karriker, and W. C. Harris, *ibid.*, **52**, 6096 (1970).

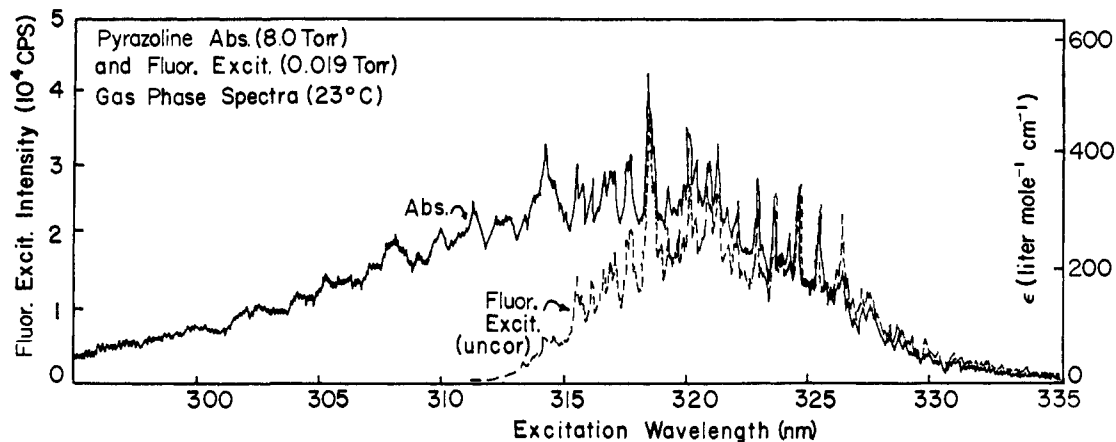


Figure 1. Gas-phase absorption spectra (8.0 Torr, 1 Å resolution) and fluorescence excitation spectra (0.019 Torr,  $\sim 0.3$  Å resolution) of 1-pyrazoline. The intensities of the excitation spectra (uncorrected for spectral sensitivity) are in arbitrary units.

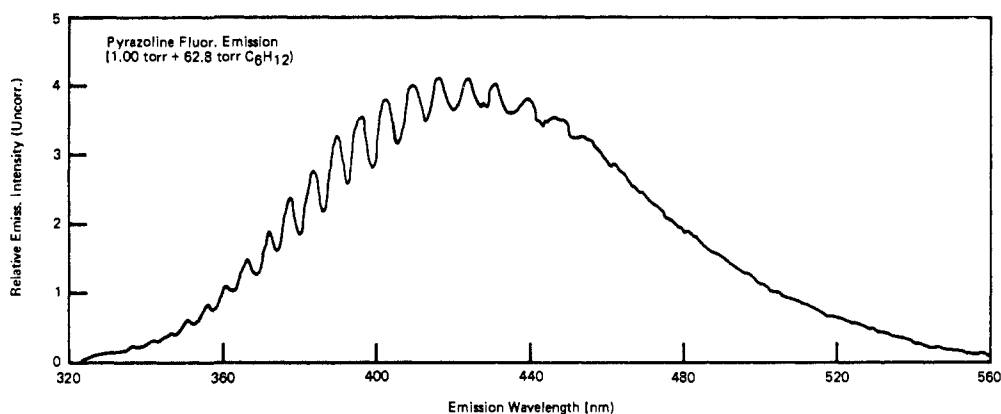


Figure 2. Fluorescence emission spectra of 1-pyrazoline (10 Å resolution).

treating this  $C_s$  ring symmetry as a small perturbation on the  $C_{2v}$  local symmetry of the azo group. The relative energies and transition moments for 1-pyrazoline thus should be approximated by those calculated by Robin, *et al.*,<sup>15</sup> for  $c$ -HN=NH using a gaussian orbital basis set with limited configuration interaction. Their results indicate that it is likely that the first absorption band in 1-pyrazoline corresponds to the  $\pi^* \leftarrow n$  ( ${}^1B_2 \leftarrow {}^1A_1$ ) transition while the second belongs to the  $\sigma^* \leftarrow n$  ( ${}^1B_1 \leftarrow {}^1A_1$ ) transition.

The absorption and high resolution excitation spectra obtained for gaseous 1-pyrazoline in this longer wavelength region are presented in Figure 1. Since no simple vibrational progressions are apparent upon inspection of this band it probably includes many hot-band transitions.

The high resolution excitation spectrum of 0.019 Torr of 1-pyrazoline (Figure 1) closely resembles the absorption spectrum at low excitation energies but falls off rapidly at higher excitation energies. Emission becomes very weak by 312 nm and is no longer detectable upon excitation at wavelengths shorter than 308 nm in the first absorption band. The lines in the first absorption band are noticed to become increasingly more diffuse as the excitation wavelength approaches and then becomes shorter than  $\sim 312$  nm.

As will be apparent later, an excited 1-pyrazoline

(15) M. B. Robin, R. R. Hart, and N. A. Kuebler, *J. Amer. Chem. Soc.*, 89, 1564 (1967).

molecule in the presence of 62.8 Torr of added cyclohexane should undergo numerous collisions during its radiative lifetime. The broad emission band in Figure 2 is thus thought to only include transitions from the vibrationally deactivated  $S_1$  state of 1-pyrazoline. If this is the case, an approximate value for the 0-0 transition of 1-pyrazoline will be given by the onset of the emission profile near  $322.9 \pm 1.3$  nm. It is of interest to note that this emission band exhibits strong vibrational structure on its short wavelength side that gradually diminishes in intensity with increasing wavelength. The separation of the peaks in this vibrational progression is  $413 \pm 17$   $\text{cm}^{-1}$  which is close to  $428$   $\text{cm}^{-1}$  assigned from vibrational spectra to the N=N ring twisting fundamental of 1-pyrazoline.<sup>14</sup>

**Quantum Yield for Emission.** Because of the many experimental difficulties involved in the direct measurement of absolute quantum yields of emission, we have resorted to measuring the relative quantum yield of emission of 0.019 Torr of 1-pyrazoline as a function of excitation wavelength,  $\phi_{F,rel}(\lambda)$ . This quantity is easily obtained by dividing the fluorescence counts at various excitation wavelengths in the excitation spectra by their corresponding values of molar extinction coefficients,  $\epsilon_\lambda$ , obtained from absorption spectra. These  $\phi_{F,rel}(\lambda)$  values have then been put on an absolute basis (designated by  $\phi_F$ ) by comparison to acetone whose emission profile is quite similar to that of 1-pyrazoline and whose fluorescence emission yield in the gas phase

is known.<sup>16,17</sup> The quantum yield of fluorescence emission of acetone has been found to change little in the wavelength range 280–313 nm and in the pressure range of 25–200 Torr with added oxygen at 40°. An absolute quantum yield of  $0.095 \pm 0.008$  at 0.030 Torr of 1-pyrazoline excited at 320 nm was thus obtained by comparing its integrated emission intensity with that of 181 Torr of acetone and 10.0 Torr of added oxygen excited at 313 nm. Corrections were made for variations in the incident light intensity at 313 and 320 nm. The band pass employed at each of these wavelengths was 1.5 nm. The  $\phi_F(\lambda)$  values are summarized in Table I.

**Table I.** Observed Lifetimes and Fluorescence Quantum Yields of 1-Pyrazoline at 23°

$\lambda_{\text{ex}}$ , nm	Excitation bandpass, nm	Pressure of 1-pyrazoline, Torr	$\tau_F$ , nsec	$\phi_F^a$
335.0	2.2	0.038	195	0.15
333.0	2.2	0.023	189	0.15
331.0	2.0	0.038	188	0.15
328.0	2.0	0.038	172	0.14
323.0	2.0	0.038	165	0.12
320.0		0.030		$0.095 \pm 0.008^b$
318.0	3.2	0.038	120	0.077
316.2	3.2	0.014	80	0.055
315.2	3.2	0.014	55	0.042
313.0	3.2	0.014	25	0.016
312.0	3.2	0.014	10	0.004

<sup>a</sup> Primarily because of the very small emission intensity, the uncertainty in the relative fluorescence quantum yield measurements near the onset of absorption is as much as  $\pm 25\%$ . Also, the uncertainty in the measurement of  $\phi_F(313)$  is  $\pm 30\%$ , and  $\phi_F(312)$  is known to within a factor of 2. <sup>b</sup> The uncertainty tabulated indicates the reproducibility of the measurement of  $\phi_F(320)$  relative to acetone emission.

**Emission Lifetimes.** These results obtained for the emission lifetimes ( $\tau_F$ ) of 1-pyrazoline at various excitation wavelengths are also presented in Table I. Since we wished to study the emission properties of the 1-pyrazoline molecules in their collisionally unperturbed states and because the emission lifetimes approached 200 nsec at long wavelengths of excitation, it became necessary to employ the lowest possible pressures in our quantum yield and lifetime measurements. The mean collision frequency between 1-pyrazoline in its first excited singlet state,  $C_3H_6N_2(S_1^*)$ , and its ground state,  $C_3H_6N_2(S_0)$ , at room temperature and the highest pressure employed in either the quantum yield or lifetime measurements (0.038 Torr) is  $\sim 7.6 \times 10^5 \text{ sec}^{-1}$ . Thus at the longest wavelengths of excitation, on the order of 13% of the  $C_3H_6N_2(S_1^*)$  could have been collisionally perturbed prior to fluorescence. The emission decay in the shorter wavelength region ( $\lambda_{\text{ex}} \leq 313 \text{ nm}$ ) is nonexponential. In this region the initial slopes were used to calculate  $\tau_F$ . This nonexponential behavior is very probably due to the preparation of several vibronic states because of the relatively wide bandpass used for excitation. However, an alternate explanation of the nonexponential decay curves might be that in this shorter wavelength region in which  $\tau_F$  is decreasing rapidly, intramolecular energy relaxation might be

(16) R. G. Shortridge, C. F. Rusbult, and E. K. C. Lee, *J. Amer. Chem. Soc.*, **93**, 1863 (1971).

(17) J. Heicklen, *ibid.*, **81**, 3863 (1959).

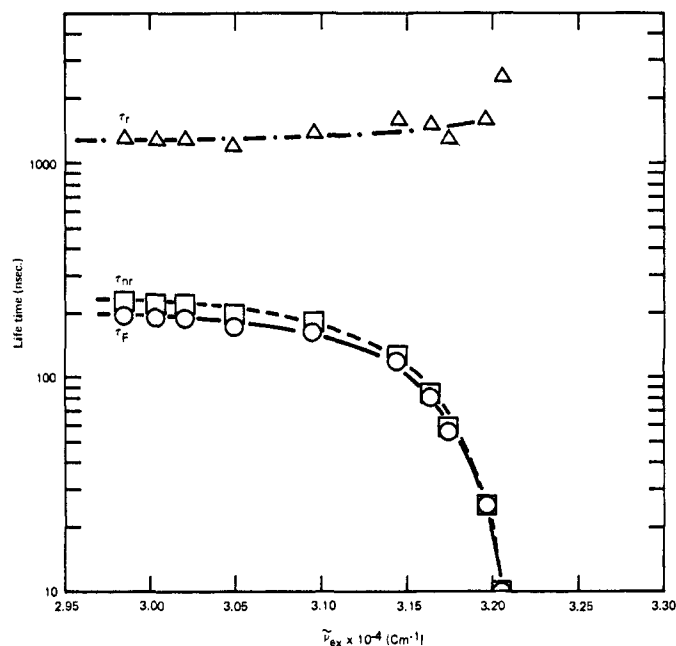


Figure 3. The measured fluorescence decay lifetime,  $\tau_F$  (O), radiative lifetime,  $\tau_r$  ( $\Delta$ ), and nonradiative lifetime,  $\tau_{nr}$  ( $\square$ ), as a function of excitation energy.

faster than decay of the singlet state, and the observed emission could be from several vibronic states with different lifetimes.<sup>18</sup>

The radiative and nonradiative lifetimes of 1-pyrazoline ( $\tau_r$  and  $\tau_{nr}$ ) have been estimated by use of the following expressions.

$$\tau_r = \tau_F / \phi_F \quad (2)$$

$$\tau_{nr} = \tau_F / (1 - \phi_F) \quad (3)$$

The values of  $\tau_r$  and  $\tau_{nr}$  obtained from the values of  $\tau_F$  and  $\phi_F$  given in Table I are plotted in Figure 3 along with the measured  $\tau_F$  values as a function of excitation frequency  $\tilde{\nu}_{\text{ex}} = 1/\lambda_{\text{ex}}$ . The radiative lifetime calculated from the Strickler–Berg<sup>19</sup> expression using the integrated absorption coefficients is 1100 nsec. Calculations of radiative lifetimes for transitions of this nature are only of order of magnitude validity.<sup>19,20</sup>

**Quantum Yield for Decomposition.** By measurement of the relative amounts of products formed on photolysis by 313-nm radiation of mixtures of 1.48 Torr of 1-pyrazoline and 17.9 Torr of cyclobutanone, the quantum yield for decomposition of 1-pyrazoline,  $\phi_D(313)$ , was found to be  $0.7 \pm 0.1$ . An experiment in which 2.84 Torr of 1-pyrazoline and 10.4 Torr of cyclobutanone were photolyzed separately gave  $\phi_D(313) = 1.08$ . These results are based on values of  $4.4 \text{ l. mol}^{-1} \text{ cm}^{-1}$  for  $\epsilon_{313}$  of cyclobutanone,<sup>11</sup> and  $276 \text{ l. mol}^{-1} \text{ cm}^{-1}$  for  $\epsilon_{313}$  of 1-pyrazoline.

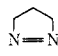
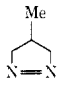
In a following section we illustrate the pressure dependence of  $\phi_F(313)$  with cyclohexane as the diluent gas. We find that at a total pressure of 20 Torr of cyclohexane  $\phi_F(313)$  is  $\sim 0.1$ , and at 2.8 Torr  $\phi_F$  is  $\sim 0.06$ . Assuming that the collisional efficiencies of cyclohexane, cyclobutanone, and 1-pyrazoline do not differ significantly, the results indicate that at shorter

(18) S. H. Lin, *J. Chem. Phys.*, **56**, 4155 (1972).

(19) S. J. Strickler and R. A. Berg, *ibid.*, **37**, 814 (1962).

(20) B. S. Solomon, T. F. Thomas, and C. Steel, *J. Amer. Chem. Soc.*, **90**, 2249 (1968).

Table II. The Product Composition Resulting from the Photochemical Decomposition of 1-Pyrazoline and 4-Methyl-1-pyrazoline

Reactant	Excitation	Total pressure, Torr	Cyclopropane + propene		Ethylene
	333 nm	≥ 3 + 10 (O <sub>2</sub> ) <sup>a</sup>	98.4		1.6
	333 nm	≥ 10	97.4		2.6
	333 nm	≤ 0.10	90		10
	313 nm	≤ 0.30	82		18
Methyl-					
	330 nm 313 nm Hg (253.7 nm)	> 50 ≤ 0.25 320 (N <sub>2</sub> )	Methyl-	Isobutene	Propene
			cyclopropane <sup>b</sup>		
			66	29	5
			77	9	14
	93	4	3		

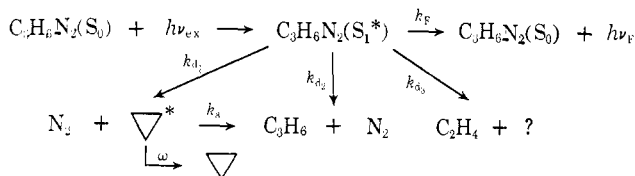
<sup>a</sup> See caption to Figure 6 for explanation. <sup>b</sup> The relative amount of products formed in the primary process is tabulated. The vibrationally excited methylcyclopropane isomerizes to the butene isomers unless it is collisionally stabilized by the bath molecules. At lower pressures the relative amount of methylcyclopropane formed in the primary process is calculated from the sum of the observed methylcyclopropane plus the butene isomers to which some of it has isomerized (ref 7).

wavelengths of excitation there is no important non-radiative path of depopulation of the excited singlet state that does not lead to fragmentation.

The average of three experiments in which the quantum yield for decomposition of 1-pyrazoline excited by 333 nm radiation was measured relative to  $\phi_D(313)$  is  $0.59 \pm 0.05$ . Comparison of this value with the value for  $\phi_F(333)$  (Table I) illustrates that on excitation near the onset of absorption to the first singlet state the sum,  $\phi_F(333) + \phi_D(333)$ , is  $0.74 \pm 0.10$ . Since the fluorescence emission profile is unchanged by adding oxygen (the intensity decreases equally at all emission wavelengths), it is unlikely that 1-pyrazoline phosphoresces. The results imply that near the onset of absorption to the first singlet state there is a non-radiative path that does not lead to fragmentation. However, because of the relatively large error associated with the measurements of  $\phi_D$ , and particularly  $\phi_F$ , in this region of  $\lambda_{ex}$  (Table I), this is not particularly strong evidence for such a process. Also, since  $\phi_F$  is a relative measurement, any error in the fluorescence quantum yield for acetone would be reflected in the present measurements.

**Discussion of the Primary Processes in 1-Pyrazoline Photolysis.** The product compositions produced on photolysis of 1-pyrazoline in the lower and higher pressure regions are summarized in Table II. The 1-pyrazoline photolysis in the absence of a singlet state quenching diluent is described in Scheme I, where  $\omega$  is the collisional

#### Scheme I



sional vibrational deactivation rate of the vibrationally excited cyclopropane, CP\*, produced on photodecomposition of 1-pyrazoline. The data contained in Table I and Figure 3 illustrate that for  $\lambda_{ex} > 315$  nm  $k_F$  is independent of excitation energy, but the sum of the dissociative rate constants increases with increasing vibrational excitation in the singlet state. Because vibrational deactivation by collision of the initially prepared singlet state ( $S_1^*$ ) is relatively efficient (see the following section), the quantum yields for fluorescence and de-

composition, and the average energy of the decomposing singlet state, are pressure dependent.

Recent theoretical arguments have been advanced which illustrate that the nonradiative lifetime of an excited singlet state is a function of the vibrational quantum number of a dominant high frequency promoting mode.<sup>21,22</sup> In general, if the singlet-triplet energy gap is sufficiently large the intersystem crossing rate should increase with increase in the vibrational energy of the decaying singlet state. Since  $\tau_{nr}$  begins to fall off at quite low  $\lambda_{ex}$  (within 500 cm<sup>-1</sup> above the 0-0 transition), the data presented here are not of high enough resolution to extract much detail about vibrational modes that might play an important role in intersystem crossing. However, the energy dependence of  $\tau_{nr}$  indicates that intersystem crossing is a possible route for depletion of the  $S_1$  state.<sup>21</sup>

Some insight into the nature of the dissociation process is offered by the product composition data (Table II). The cleavage reaction to produce olefins (ethylene in the present case) is a stereospecific singlet state reaction of 1-pyrazolines.<sup>1-3</sup> The data in Table II indicate that the rate of cleavage increases at lower pressures and shorter  $\lambda_{ex}$ ; therefore, the decrease in  $\tau_{nr}$  is at least in part due to an increased dissociative rate from a singlet state. However, the product compositions resulting from the photolysis of *cis*- and *trans*-3,4-dimethyl-1-pyrazolines<sup>3</sup> indicate that dissociation from a triplet state becomes more important as  $\lambda_{ex}$  decreases. Consistent with that observation is that the unique 1,2-hydrogen migration product, isobutene, formed in the primary photodissociation of 4-methyl-1-pyrazoline becomes less important on photolysis at higher energies (Table II). The 1,2-hydrogen migration product is typically a minor product, if produced at all, in the triplet sensitized decomposition of 1-pyrazolines.<sup>1-3</sup> A detailed study of the photochemistry of the dimethyl-1-pyrazolines should offer more insight about the possible importance of intersystem crossing in 1-pyrazoline photolysis.

**Vibrational Deactivation of the Excited Singlet State of 1-Pyrazoline.** Vibrational deactivation by collision with unreactive molecules enhances the fluorescence of 1-pyrazoline. In the absence of a singlet state quenching diluent one can, by including collisional vibrational

- (21) A. Nitzan and J. Jortner, *J. Chem. Phys.*, **55**, 1355 (1971).  
 (22) A. D. Brailsford and T. Y. Chang, *ibid.*, **53**, 3108 (1970).

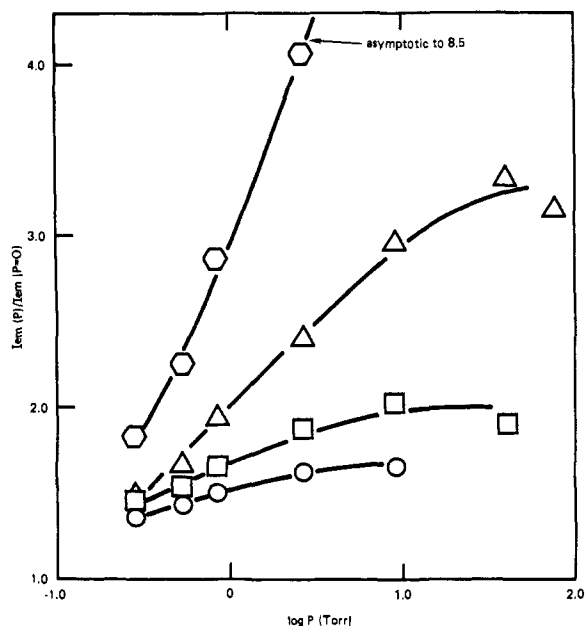


Figure 4. The relative fluorescence emission intensity of 0.028 Torr of 1-pyrazoline as a function of cyclohexane diluent pressure for several representative  $\lambda_{\text{ex}}$ : 333 nm ( $\circ$ ); 323 nm ( $\square$ ); 315.6 nm ( $\Delta$ ); 313 nm ( $\diamond$ ). The excitation spectra bandpass is 2.0 nm.

deactivation of the initially prepared singlet state,  $S_1^*$ , in Scheme I, derive the relationship 4, which describes the

$$\frac{I_{\text{em}}(\omega_e)}{I_{\text{em}}(\omega_e = 0)} = \frac{1}{1 + \tau_F(\lambda)\omega_e}(1 + \tau_F(\text{max})\omega_e) \quad (4)$$

emission intensity as a function of the vibrational deactivation rate,  $\omega_e$ . In eq 4  $\tau_F(\lambda)$  and  $\tau_F(\text{max})$  are the measured (Table I) singlet state lifetimes in the collision-free region at the appropriate value of  $\lambda_{\text{ex}}$ , and the high pressure limiting value for  $\tau_F$  (308 nsec), respectively. In Figure 4 we illustrate the pressure dependence of the emission intensity with cyclohexane as a diluent for several representative values of  $\lambda_{\text{ex}}$ . Application of eq 4 to the data for  $\lambda_{\text{ex}}$  = to 333, 331, 328, and 323 nm gives

$$\omega_e = 2.1 \pm 0.2 \times 10^7 \text{ sec}^{-1} \text{ Torr}^{-1}$$

This result is about equal to the gas kinetic collision rate calculated using estimated Lennard-Jones collision parameters.<sup>23</sup>

The efficiency of cyclohexane as a vibrational deactivator appears to decrease if the pyrazoline is excited by wavelengths shorter than  $\sim 320$  nm. In the region in which  $\tau_{\text{nr}}$  is falling off quite rapidly with increased energy of excitation it is likely that the effect of "upjumps" to produce sufficiently excited singlet state molecules that cannot be trapped by successive collisions is becoming apparent.

Although we have not carefully documented its efficiency as a vibrational deactivator, we do find that the lifetime of the singlet state of 1-pyrazoline approaches 320 nsec as its own pressure is raised to 7.5 Torr. Moreover, lifetime measurements in which 1 Torr of 1-pyrazoline with various higher pressures of cyclohexane added also resulted in  $\tau_F$  reaching  $\sim 320$  nsec at higher diluent pressures. Both of these series of experiments

(23) J. O. Hirschfelder, C. F. Curtis, and R. B. Bird, "Molecular Theory of Gases and Liquids," Wiley, New York, N. Y., 1954.

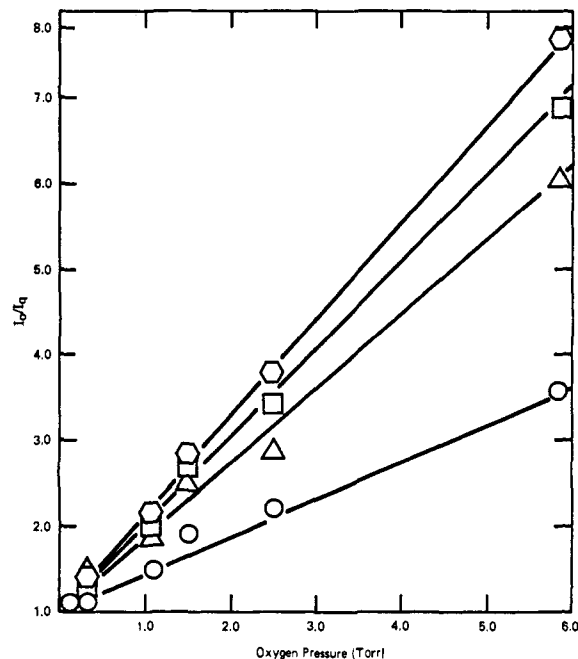


Figure 5. Oxygen quenching of 1-pyrazoline (0.024 Torr) fluorescence for several representative  $\lambda_{\text{ex}}$ : 328 nm ( $\circ$ ); 320.5 nm ( $\square$ ); 318 nm ( $\Delta$ ); 313 nm ( $\diamond$ ). The excitation spectra bandpass is 1.5 nm.

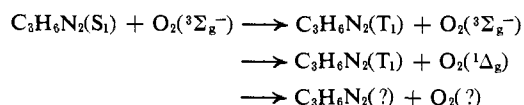
indicate that self quenching is not an important process in 1-pyrazoline photolysis.

**Oxygen Quenching of Singlet 1-Pyrazoline.** Oxygen is a very efficient quencher of 1-pyrazoline fluorescence. In Figure 5 we illustrate the steady-state emission intensities in the presence,  $I_q$ , and in the absence,  $I_o$ , of oxygen for several  $\lambda_{\text{ex}}$ . From the relationship

$$I_o/I_q = 1 + \tau_F(\lambda)k_q[\text{O}_2] \quad (5)$$

where  $\tau_F(\lambda)$  is the measured singlet state lifetime at the appropriate  $\lambda_{\text{ex}}$  (Table I), and from the data illustrated in Figure 5 we calculate the value of  $k_q$ , the bimolecular quenching rate constant for oxygen quenching of 1-pyrazoline fluorescence, to be  $1.2 \times 10^{11} \text{ l. mol}^{-1} \text{ sec}^{-1}$ , independent of  $\lambda_{\text{ex}}$  down to 318 nm. The quenching data for shorter  $\lambda_{\text{ex}}$  are not reliable because of the uncertainty in  $\tau_F$ . The collision between cross section  $\pi\sigma^2$  for oxygen quenching is  $37 \text{ \AA}^2$ , which implies a collision efficiency of  $\sim 0.5$ .<sup>23</sup> The efficiency of oxygen quenching of 1-pyrazoline fluorescence is at least as great as its efficiency for the quenching of the excited singlet states of aromatics. In the latter case charge transfer quenching has been proposed as a mechanism.<sup>24</sup> The efficiency of oxygen for quenching the fluorescence of 1-pyrazoline certainly indicates that a spin-allowed, exoenergetic, process is involved.

Since the triplet energy of 1-pyrazoline is between 68 and 54 kcal mol<sup>-1</sup>,<sup>1,25,26</sup> the possible reactions are



Some insight into the nature of the pyrazoline product produced on quenching of the singlet state by oxygen

(24) T. Brewer, *J. Amer. Chem. Soc.*, **93**, 755 (1971), and references cited therein.

(25) W. D. K. Clark and C. Steel, *ibid.*, **93**, 6347 (1971).

(26) P. S. Engel, *ibid.*, **91**, 6903 (1969).

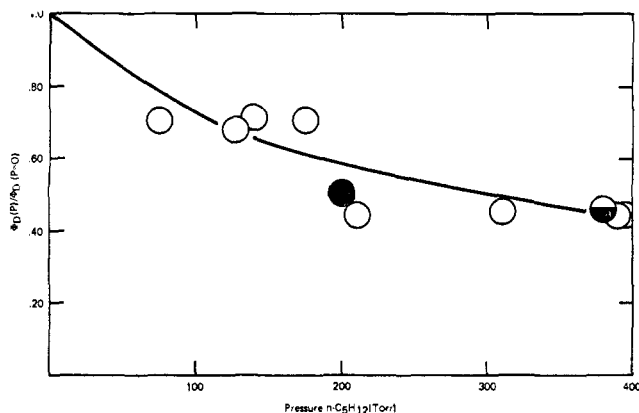
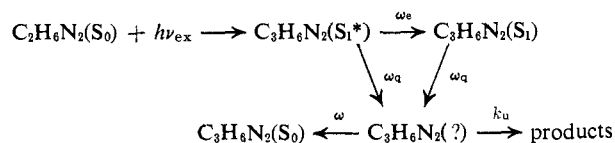


Figure 6. The relative quantum yield for decomposition of 1-pyrazoline excited by 333-nm radiation with oxygen present as a function of *n*-pentane diluent pressure: 10 Torr of oxygen added (○); 18 Torr of oxygen added (◐); 40 Torr of oxygen added (●). The solid line is a calculated curve with  $k_{\mu} = 7.0 \times 10^9 \text{ sec}^{-1}$  (see text).

can be gained from the pressure dependence of  $\phi_D$ . On excitation by 333-nm radiation in the absence of oxygen  $\phi_D(333 \text{ nm}) \approx 0.50$ , and, above  $\sim 10$  Torr of total pressure,  $\phi_D$  is independent of pressure to at least 325 Torr. However, we find that on adding 10 Torr of oxygen  $\phi_D(333 \text{ nm}) = 1.0$ . In Figure 6 we have illustrated how  $\phi_D(333)$  decreases on adding pentane when 10 Torr of oxygen also has been added to the system. These data indicate that oxygen quenching of the singlet state yields a vibrationally excited product that can be deactivated by *n*-pentane. We find that oxygen itself is  $\lesssim 0.5$  as efficient as *n*-pentane in deactivating the intermediate.

Since 10 Torr of  $\text{O}_2$  will effectively quench  $>90\%$  of the excited singlet states produced by 333 nm excitation, Scheme II is appropriate for describing the processes

#### Scheme II



that occur when the photolysis is carried out with this much oxygen and an effective vibrational deactivator diluent both present in the system. Assuming unit efficiency for vibrational deactivation of  $\text{S}_1^*$  and the quenched singlet state product by *n*-pentane,<sup>27</sup>  $\omega_e$  and  $\omega$ , respectively, and knowing the magnitude of the quenching rate,  $\omega_q$ , of the singlet state by oxygen from the relative fluorescence intensity measurements, we can calculate the magnitude of  $k_u$ , the unimolecular rate constant for decomposition of the vibrationally excited 1-pyrazoline produced by quenching of the  $\text{S}_1$  state by oxygen.

$$\phi_D \approx \frac{\omega_q}{\omega_e + \omega_q} \frac{k_u}{k_u + \omega} \left( 1 + \frac{\omega_c}{\omega_q} \right) \quad (6)$$

The value of the unimolecular rate constant,  $k_u$ , that best fits the experimental data is  $7.0 \pm 1.6 \times 10^9 \text{ sec}^{-1}$  (Figure 6).

Using the known frequency assignment<sup>14</sup> and kinetic parameters for ground-state 1-pyrazoline decomposition,<sup>28</sup> we carried out RRKM calculations<sup>29,30</sup> on the rate of decomposition as a function of excess vibrational excitation in ground-state 1-pyrazoline. These calculations indicate that the intermediate produced on quenching of the  $\text{S}_1$  state of 1-pyrazoline by oxygen contains  $\sim 55 \text{ kcal mol}^{-1}$  of internal energy. It appears that the oxygen removes about  $30 \text{ kcal mol}^{-1}$  of energy on quenching the  $\text{S}_1$  state of 1-pyrazoline, certainly enough to produce  $\text{O}_2(^1\Delta_g)$ . If oxygen quenching of the  $\text{S}_1$  state yields 1-pyrazoline in its  $\text{T}_1$  state, these results indicate that there may be rapid  $\text{T}_1 \rightarrow \text{S}_0$  inter-system crossing, and then dissociation. A similar study using the dimethyl-1-pyrazoline isomers should prove to be very helpful in elucidating the nature of the mechanism of oxygen quenching in these systems.

**Energy Partitioning on Photolysis of 1-Pyrazoline.** We have carried out a careful analysis of the product composition produced on photolysis of 1-pyrazoline as a function of diluent pressure for two photolysis wavelengths, 313 and 333 nm. The magnitude of the unimolecular rate constant,  $k_a$ , for isomerization of vibrationally excited cyclopropane produced on photolysis of 1-pyrazoline is given by

$$k_a = \omega \left( \frac{\text{C}_3\text{H}_6/\nabla - k_{a2}/k_{a1}}{1 + k_{a2}/k_{a1}} \right) \quad (7)$$

where  $\text{C}_3\text{H}_6/\nabla$  is the experimentally observed product ratio. The ratio  $k_{a2}/k_{a1}$  was determined from the limiting high pressure  $\text{C}_3\text{H}_6/\nabla$  ratio. This ratio is wavelength dependent;  $k_{a2}/k_{a1}$  is 0.19 and 0.30 for photolysis by 313-nm<sup>9</sup> and 333-nm radiation, respectively.

The experimentally determined values for  $k_a$  are illustrated in Figures 7 and 8. For both wavelengths of photolysis  $k_a$  exhibits considerable pressure dependence. The striking result is that the rate constant for  $\text{CP}^*$  isomerization is considerably greater when it is produced by photolysis of the 1-pyrazoline at the longer wavelength. The internal energy content of the  $\text{CP}^*$  may be deduced from the experimental data by noting that the observed rate constant is related to the microscopic unimolecular rate constant for isomerization of a vibrationally excited cyclopropane with internal energy  $E$ ,  $k_E$ , by<sup>6-9</sup>

$$k_a = \omega \frac{\sum \frac{k_E}{k_E + \omega} f(E)}{\sum \frac{\omega}{k_E + \omega} f(E)} \quad (8)$$

where  $f(E)$  is the internal energy distribution function of the initially formed  $\text{CP}^*$ .

We assume that  $f(E)$  has the form of a Gaussian and calculate  $k_E$  using the RRKM rate formulation<sup>7,29,30</sup> to evaluate eq 8. The calculated values of  $k_a$  that best fit the experimental data are also illustrated in Figures 7 and 8. We find that the most probable energy of the  $\text{CP}^*$  formed by 313-nm photolysis of 1-pyrazoline is  $\sim 14 \text{ kcal mol}^{-1}$  less than the most probable energy of the  $\text{CP}^*$  formed by 333-nm photolysis. The data indicate that lower pressures or greater  $E_{\text{ex}}$  results in less

(28) R. J. Crawford and A. Mishra, *J. Amer. Chem. Soc.*, **88**, 3963 (1966).

(29) R. A. Marcus, *J. Chem. Phys.*, **20**, 359 (1952).

(30) G. Z. Whitten and B. S. Rabinovitch, *ibid.*, **38**, 2466 (1963).

(27) G. H. Kohlmaier and B. S. Rabinovitch, *J. Chem. Phys.*, **38**, 1962 (1963); **38**, 1709 (1963); D. W. Setser, B. S. Rabinovitch, and J. W. Simons, *ibid.*, **40**, 1751 (1964).

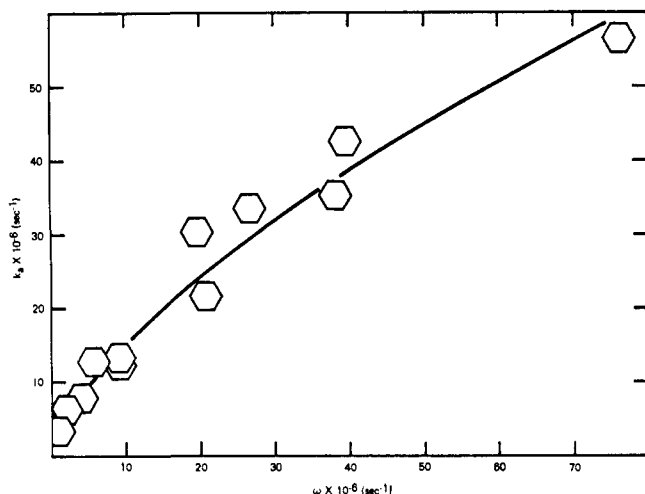


Figure 7. The experimental values of  $k_a$  as a function of  $\omega$  for  $\lambda_{ex} = 313$  nm. Propane is the diluent. The solid line is a calculated curve with  $E_{mp} = 76$  kcal mol $^{-1}$  and  $\sigma = 12$  kcal mol $^{-1}$ . These data are taken from the M.A. Thesis of A. Squillace, California State University—Fullerton, 1971.

energy being partitioned to the internal degrees of freedom of the hydrocarbon fragment.

Using the known frequency assignment<sup>14</sup> and thermal kinetic parameters<sup>28</sup> for 1-pyrazoline one may calculate the internal energy distribution function of the CP\* if there were statistical intramolecular energy relaxation<sup>8,31</sup> when 1-pyrazoline fragments to trimethylene and nitrogen. If  $\lambda_{ex}$  were 333 nm, statistical intramolecular energy relaxation would result in a cyclopropane with a most probable energy of  $\sim 86$  kcal mol $^{-1}$  (assuming that the reaction trimethylene  $\rightarrow$  cyclopropane is 54 kcal mol $^{-1}$  exothermic<sup>32</sup>). It appears that at longer

(31) F. H. Dorer and S. N. Johnson, *J. Phys. Chem.*, **75**, 3651 (1971).  
 (32) H. E. O'Neal and S. W. Benson, *ibid.*, **72**, 1866 (1968).

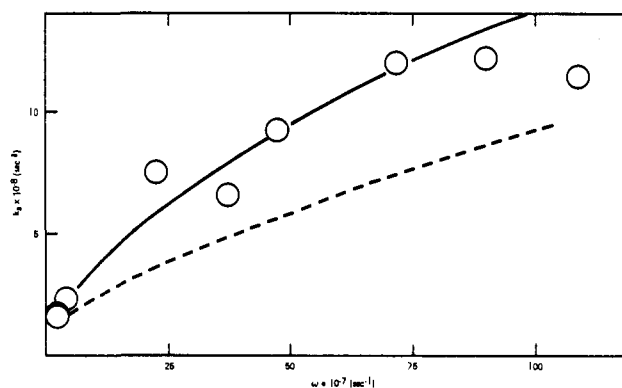


Figure 8. The experimental values of  $k_a$  as a function of  $\omega$  for  $\lambda_{ex} = 333$  nm. *n*-Pentane is the diluent. The solid line is a calculated curve with  $E_{mp} = 91$  kcal mol $^{-1}$  and  $\sigma = 15$  kcal mol $^{-1}$ . The broken line is a calculated curve with  $E_{mp} = 86$  kcal mol $^{-1}$  and  $\sigma = 12$  kcal mol $^{-1}$ .

wavelengths of excitation there is approximately statistical intramolecular energy relaxation on fragmentation. However, photolysis in the shorter wavelength region of the first singlet band, where  $\tau_{nr}$  is decreasing with increased excitation energy, results in a nonrandom distribution of the available energy. In the short wavelength region more of the available energy is partitioned to degrees of freedom other than the internal degrees of freedom of the hydrocarbon fragment.

**Acknowledgments.** This work has been supported in part by the National Science Foundation Grant No. GP-28266. We wish to express our gratitude to Professor E. K. C. Lee of the University of California—Irvine for allowing us to use the facilities in his laboratory to carry out the fluorescence emission and lifetime studies, and for his interest in this work. We also thank M. Ezell and A. Squillace for their contributions during the initial stages of this study.

## Electron Spin Resonance Study of Heterocycles.

### II. Pyrrole, Pyrazole, Imidazole, and Indole Anion Radicals<sup>1</sup>

Paul H. Kasai\* and D. McLeod, Jr.

Contribution from the Union Carbide Corporation, Tarrytown Technical Center, Tarrytown, New York 10591. Received June 28, 1972

**Abstract:** Anion radicals of pyrrole, pyrazole, imidazole, and indole were generated in argon matrices, and their esr spectra were examined. For pyrrole, pyrazole, and imidazole, the anion radicals were found to exist in their tautomeric  $\alpha$ -pyrrolenine form, e.g., **2** as shown in the text. In the case of indole anion, the N-H proton was found to transfer to the benzene ring giving rise to the anion radical of the form VII (see text).

Early studies of pyrroles noted the similarity between the chemistry of pyrroles and phenols. The noted similarity was initially attributed to their tautomerism: IA  $\rightleftharpoons$  IB and IIA  $\rightleftharpoons$  IIB. Subsequent studies, however, showed that neither phenol nor pyrrole exists in its keto (IB) or imine (IIB) tau-

(1) For an account on pyridyl radicals, see P. H. Kasai and D. McLeod, Jr., *J. Amer. Chem. Soc.*, **94**, 720 (1972).

meric form. The similarity of the chemistry is now understood in terms of the positive charge imparted into the resonating  $\pi$  orbitals by the electro-negative heteroatoms.<sup>2</sup>

Recently we have examined the electron spin reso-

(2) For a historic account of the comparison of the chemistry of pyrroles and phenols, see R. C. Elderfield, Ed., "Heterocyclic Compounds," Vol. 1, Wiley, New York, N. Y., 1950.